Presented at the 35th European PV Solar Energy Conference and Exhibition, 24-28 September 2018, Brussels, Belgium

IMPROVEMENT OF SOLAR CELL EFFICIENCIES FOR ULTRASHORT-PULSE LASER CONTACT OPENING WITH NI-CU PLATED CONTACTS BY OPTIMIZED LCO – FFO PROCESSING ORDER

V. Arya[1], S. Gutscher[1], S. Kluska[1], F.Meyer[1], G. Cimiotti[1], J. Nekarda[1], A. A. Brand[1]
[1]Fraunhofer Institute for Solar Energy Systems ISE
Heidenhofstr. 2, 79110 Freiburg, Germany

ABSTRACT: We demonstrate that the standard fast firing (FFO) process at temperatures around 850°C can significantly reduce the damage caused by a UV picosecond pulse laser ablation for nickel-copper plated silicon solar cells. Although, the metallization via Ni/Cu/Ag plated contacts are a promising technology, disruption in the crystalline structure of silicon due to laser pulse damage pertains, which increases recombination and suppresses the efficiency of solar cell. We realize laser openings of linewidths ~12.7 µm to ~16.9 µm for metallization by plating on semi-finished industrial PERC solar cells and demonstrate that by flipping the chain of processes from FFO followed by laser ablation (LCO) to LCO followed by FFO, significant reduction is seen in laser-damage induced recombination which increases the power conversion efficiency (η) by 0.5% $_{abs}$.

Keywords: laser ablation, recombination, annealing, c-Si, PERC, solar cell, plating

1 INTRODUCTION

Although, the technology of laser contact opening (LCO) and Ni/Cu/Ag light-induced plating for forming front side contacts could offer economic and technological advantages over the industries' standard silver screen printing, it often falls short of expectation. One of the suggested advantages of using Ni-Cu plating would be reduced production costs [1] (studies suggest that 40% of cell processing cost constitutes of silver paste costs [2]). Also, narrower metallization lines (10-30 µm) leading to smaller shading effects, lower specific contact resistivity [3]. Sufficient adhesion of the plated contacts has been demonstrated to be achievable by the surface morphology created by typical ultrafast pulse laser ablation process [4] .

Despite the progress of laser ablated and plated contacts, the resulting solar cell efficiencies (η) are often inferior to those achieved by screen printed contacts on the same solar cell structures. Crystal damage caused by the laser ablation increases recombination, lowering open circuit voltage (V_{oc}) and pseudo-fill-factor (*pFF*) keeping the LCO+Plated contacts from reaching their full efficiency potential.

Damage due to LCO of anti-reflection coatings on silicon solar cells is well researched and published. Drops in V_{oc} [5] and decrease in minority carrier lifetime [6], [7] have been reported. Primarily, amorphized silicon, dislocations cause increased recombination [8]–[10].

LCO for Ni-Cu plating on solar cell emitters demands for the residual damaged zone to be as shallow as possible. Ultrashort pulse lasers with a typical pulse duration of less than 15 ps offer a small thermal diffusion length (40-80nm). Also, optical absorption lengths of the laser radiation of less than 40nm can be achieved by frequency conversion to ultraviolet, typically 355 nm or 343 nm wavelength. Laser ablation with such parameters creates steep pressure and temperature gradients leave an amorphous silicon surface due to rapid cooling in the heat affected zone (HAZ) [9]–[11].

1.1 Recrystallization of Laser Amorphized Silicon

Attempts to improve recombination by employing KOH/NaOH etching after laser ablation has been successfully demonstrated for buried contacts [5]. However, etching away the laser-damaged silicon layer would increase production costs of LCO + Ni-Cu plated contacts. Additionally etching away the top part of the emitter with the highest doping concentration would most likely decrease the emitters' ability to shield the metal contacts and increase contact resistance.

Thermal annealing has been proven to be an effective method of transforming amorphous silicon to crystalline silicon as reported in [12]–[14]. It has been shown that annealing a-Si up to temperatures of 900°C initiates the crystallization of the a-Si layer [12]. In another study, Raman scattering spectra reveals amorphous silicon transforming to nearly fully crystallized poly-Si film after subjecting to temperatures of 700-1100°C [14].

1.2 Fast Firing Oven (FFO)

Fast Firing process (FFO) is a standard process in manufacturing crystalline silicon solar cells. Its primary purpose in the process chain is activating the passivation layer and sintering silver and aluminum pastes to form front and rear side contacts. Typical peak temperatures of the solar cells are around 850°C for several seconds. In the preparation of PERC solar cells specifically, FFO is typically the last processing step following screen printing of metal paste on both sides.

However for manufacturing PERC cells with laser ablated and plated front contacts, the wafers are often processed to the point where they have already received full area aluminum screen printing on the rear side and subsequent FFO. These PERC precursors without front side contacts are then usually subjected to front side laser LCO and plating.

In our work, we change the processing order. The wafers are subjected to front side LCO before FFO is applied in order to utilize the thermal budget of the FFO to anneal the laser damage along with rear side contact formation.

2 EXPERIMENT DESIGN

Semi-finished p-type Cz-Si monocrystalline PERC solar cells were procured for the experiment which were processed on the rear side (LCO + Al paste) but not yet fired. The front side carried KOH textured surfaces with random pyramids. A total of 200 cells were equally divided into two groups namely Group A and Group B. The Group A cells were exposed to front side laser ablation and then subjected to FFO and the process was

reversed in the Group B. The whole process flow is shown in Figure 1. It was made sure that all the cells from both the groups receive the FFO process simultaneously so both the groups receive exactly the same thermal annealing treatment.

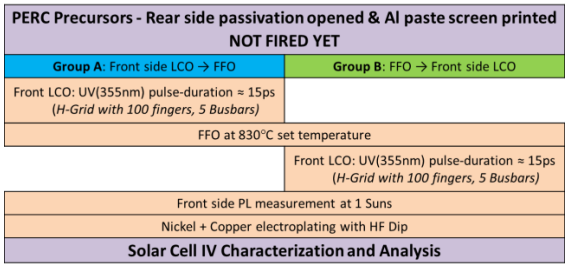

Figure 1: Process flow chart illustrating the two groups with altered process order of front side LCO before FFO (A) and FFO before front side LCO (B)

2.1 Laser Ablation of SiN_x

The laser employed for front side laser ablation is an ultrashort pulsed UV (355nm) laser with pulse-duration of < 15ps. All the cells were lasered with a complete H-Grid geometry (see Figure 2) comprised of 100 fingers, 5 busbars (each 0.5mm wide).

Both groups were divided into 5 sub-groups and they were lasered upon with five different pulse energies E_{pulse}- 0.5µJ, 0.6µJ, 0.8µJ, 0.9µJ and 1.0µJ while keeping all other laser beam characteristics constant throughout the experiment. Different pulse energies generated different opening sizes in the dielectric layer on the solar cell. The opening widths varied from ~12.5µm at 0.5µJ to ~16.9µm at 1.0µJ as shown in Figure 3. As expected, the openings at a higher pulse energy leave behind much less residue of the dielectric layer hence appear shinier. The residual dielectric layer plays its part in increasing the overall series resistance of the Ni-Cu plated solar cells as will be visible in the IV results in the subsequent sections.

After subjecting both the groups to both LCO and FFO, PL measurements were performed at one sun illumination intensity to characterize the pre-metallization lifetime performance of the cells and the effect of laser pulse energy variation on it.

2.2 Light induced Ni-Cu plating (LIP)

Following the PL characterization, they were subjected to inline Ni/Cu/Ag light-induced plating processes. The cells were dipped in 1 wt% HF solution for 30s to strip off native oxide followed by growing of nickel seed layer in the ablated areas and further received light induced copper and silver plating process. This completes the process of forming the contacts by electroplating. No anneal was performed after plating. The cells followed IV characterization.

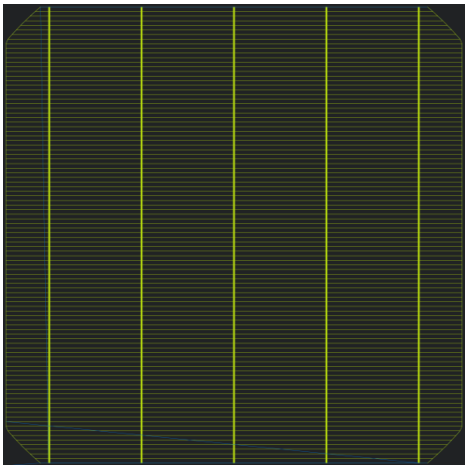

Figure 2: Schematic of an H-Grid front metallization grid geometry with 100 finger and 5 Busbars.

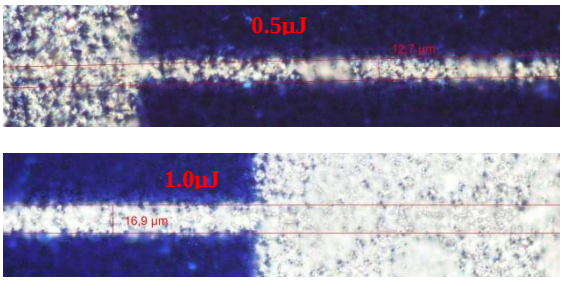

Figure 3: Laser ablated contact openings at 0.5µJ and 1.0 µJ having opening widths of 12.7µm and 16.9µm respectively. The blue part is the SiN_x dielectric film and the shining silver part is the silicon exposed after laser ablation. Openings at 0.5µJ appear cloudy and patchy due to incomplete ablation compared to opening at 1.0µJ.

3 RESULTS

3.1 Photoluminescence Measurements (PL)

PL measurements were performed on all the wafers from both the groups after they received both laser opening and once the rear side passivation was activated after FFO. Figure 4 below shows the mean PL counts of Group A cells (LCO → FFO) juxtaposed with Group B (FFO → LCO) cells at various pulse energies.

Two things can be immediately concluded from this – (i) there is general and intuitive upward trends in the PL counts with decreasing pulse energy, (ii) Group A (LCO → FFO) shows a significant improvement in the PL counts over Group B which do not receive the FFO anneal treatment after laser ablation.

3.2 IV Characterization

The non-degraded cells were subjected to standard IV characterization. A quick look at the Figure 5 directly indicates, keeping in accordance with the PL results, a significant jump in the efficiency of solar cells that received the FFO after LCO at all different laser pulse energies. An improvement of ~0.25%$_{abs}$ at higher pulse energies to >0.50%$_{abs}$ at lower pulse energy is seen in the efficiency (η) when cells are thermally annealed after LCO.

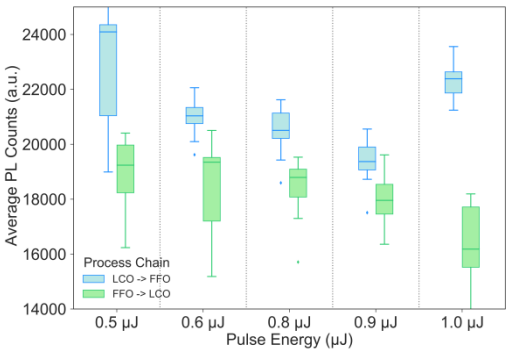

Figure 4: Mean PL counts vs. ablation pulse energy for Group A (LCO → FFO) and Group B (FFO → LCO) cells.

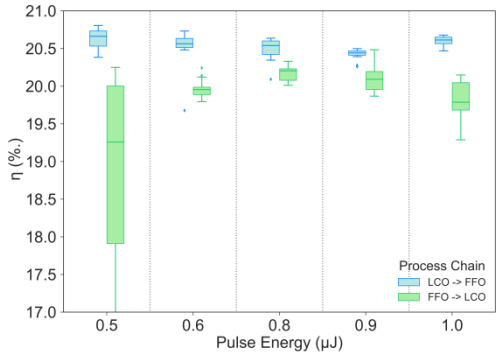

Figure 5: Solar cell efficiency η vs. laser ablation pulse energy (µJ).

3.3 FFO→LCO Process Sequence

Deeper look reveals some interesting insights into the trade-offs that are at work in case of laser + plated solar cells. Looking at the FFO→LCO order separately, we observe that the cells lasered with pulse energy of 0.8µJ demonstrate the best efficiency results, both in terms of median and the scatter of data. The efficiency of cells lasered upon with the minimum pulse energy of 0.5µJ shows a large spread on the efficiency scale indicating higher uncertainty. Even though the V_{oc} trends indicate continuous drop with increasing pulse energies, (as expected – increasing pulse energy should result in higher dislocations and recombination sites, ergo lower V_{oc}) and the j_{sc} shows hardly any significant dependence on pulse energies (see Figure 6), the efficiencies however do not slide off with increasing pulse energies, as one would have expected.

Here the quality of the contact opening, in terms of the residual dielectric layer, and the resistance it offers play a significant role. This will become much clear looking at the Fill Factor (*FF*) and pseudo-Fill Factor *(pFF)* trends of the cells. The pFF describes the fill factor of the solar cell which doesn't take into account, the drop in maximum output power (P_{mpp}) due to the series resistance (R_s) of the solar cell.

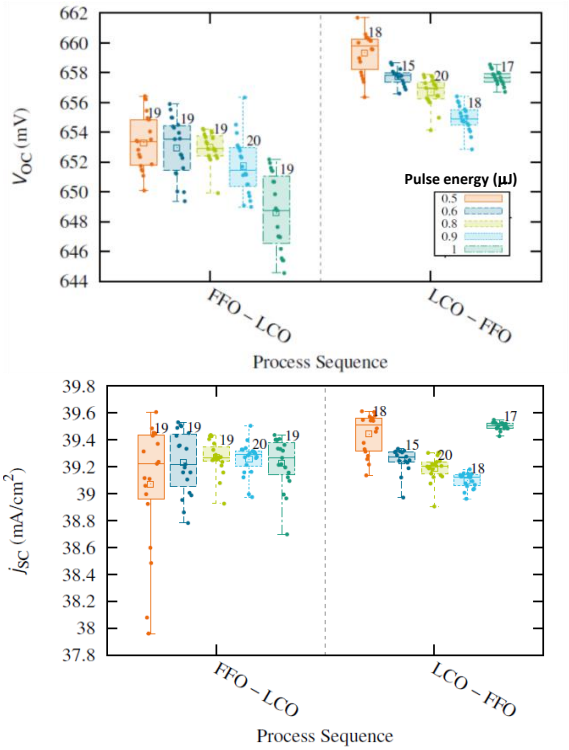

Figure 6: V_{oc} (mV) and j_{sc} (mA/cm²) at different pulse energies for the LCO → FFO and FFO → LCO process sequences.

In Figure 7, the *pFF* of the cells for FFO→LCO process is showing a downward trend with increasing pulse energies, implying higher damage (just as in case of V_{oc}). Interestingly, the downward trend of *pFF* is not seen for the LCO→FFO process and stabilization is seen with various pulse energies.

The R_s trends, as in Figure 7, show decrease in total series resistance with increasing pulse energies. This decrease in R_s is attributed to the quality of contact that the plated metal makes with the emitter in the ablated area. Presence of SiN_x residue in ablated area due to insufficient/lower pulse energies (as seen in Figure 3), indicate to be resulting in a poor or rather 'obstructed' ohmic contact which is indicated in the higher values of R_s for smaller pulse energies.

As a consequence of increasing R_s with decreasing pulse energies, the actual Fill Factor (*FF*) (see Figure 8), in disagreement with *pFF*, comes out to be highest at middle range pulse energies (0.8 & 0.9 µJ) where the amount of drop in V_{oc} is balanced out by lower series resistances. Consequently, the trade-offs between V_{oc}, R_s and *FF* churn out the highest efficiency η at 0.8µJ.

At 1µJ pulse energy, although the R_s is lowest but also the drop in V_{oc} is highest, which results in lower *FF* and hence lower overall efficiency. Contrastingly, at 0.5µJ pulse energy, the V_{oc} is the highest (ergo: high *pFF*) but so is R_s, resulting in lower *FF*. It is also notable that the larger spread of R_s at 0.5µJ pulse energy is also further transposed to a larger spread in *FF* and the end efficiency η. The large scatter in R_s values at lower pulse energies indicates inhomogeneous laser openings, with sporadic spread of residual SiN_x and irregular contacts.

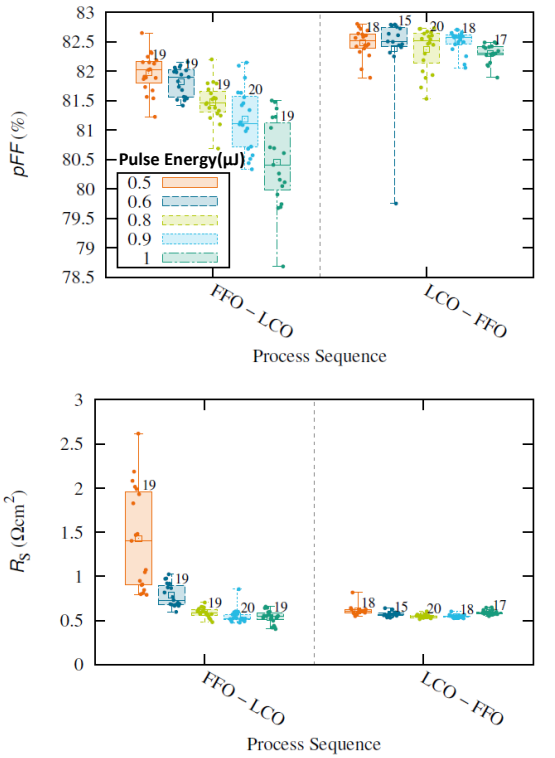

Figure 7: *pFF* (%) and R_s (Ωcm²) at different pulse energies for the LCO → FFO and FFO → LCO process sequences.

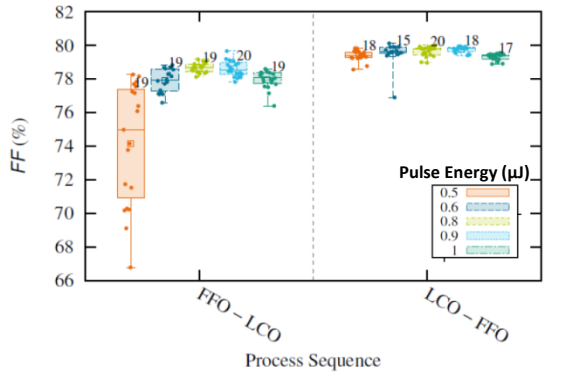

Figure 8: Fill Factor *FF* (%) at different pulse energies for the LCO → FFO and FFO → LCO process sequences.

The best cell performance is shown by cell lasered with pulse energy 0.9µJ. The efficiency measured is 20.48% with V_{oc} – 654 mV, j_{sc} – 39.33 mA /cm² & *FF* – 79.6%.

3.4 LCO→FFO Process Sequence

Thermal annealing the cells after laser process prominently show an upsurge in the average V_{oc} whilst maintaining the similar trend against pulse energy, as is clearly visible in Figure 5, compared to the reversed processing sequence. Also the *FF* stays more constant at all pulse energies (see Figure 8). Both of these factors contribute to higher solar cell efficiencies at all pulse energies and also less sensitivity of η to pulse energy.

The best cell showed an efficiency of 20.8% with V_{oc} – 660 mV, j_{sc} – 39.6mA/cm² and a *FF* of 79.6% and was lasered with the pulse energy of 0.5µJ.

3.5 High Efficiency Laser Ablated and Ni-Cu Plated Solar Cell

The new processing sequence of FFO after LCO was applied to semi-finished PERC precursors from our industrial partner Hanwha QCells GmbH.

The 156mm x 156mm pseudo square wafers featured two different emitter doping profiles namely Group B2 and Group B3. Group B2 has 100 Ω/sq. emitter profile and Group B3 has 150 Ω/sq. emitter profile with a lower surface dopant concentration. Both the groups were subjected to exactly similar laser, plating and firing processes and parameters.

The precursors were received with both sides passivated and the rear side passivation was already ablated. The front side passivation was ablated at ISE and then sent back to the industrial partner for further rear side processing. The PERCs received full area Aluminum paste screen printing on the rear side and were subsequently fired (FFO). The front side Ni-Cu plating was further performed at ISE by Kluska et al [15].

Front side screen printed (with Ag paste) metal grid PERCs were taken as reference cells for performance comparison. The screen printing of the front metal fingers was performed using 30µm screen opening. In both the cases (screen printing and laser ablation), 114 fingers and 6 busbars were applied on the front side of cells.

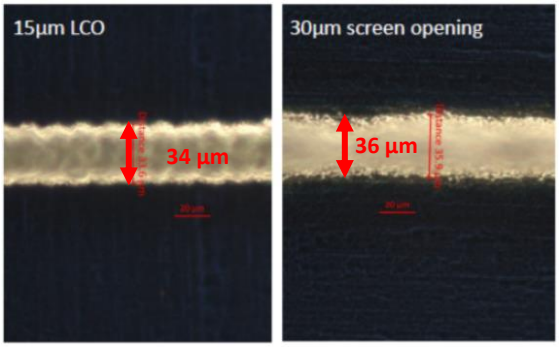

Figure 9: Metallized fingers of cells. The left image show Ni-Cu plated fingers on LCO openings of width 15µm. After plating, the fingers are ~34µm wide. The right image shows ~36µm wide screen printed finger of cells which were used as reference.

A certain pulse energy was chosen for the front side laser ablation such that the finger openings were approximately 15µm wide. The finger width after Ni-Cu plating come about to be around 35µm wide. This was done on purpose in order to have a suitable comparison with screen printed reference cells which also bear ~35µm wide fingers (see Figure 9). A highlight of the best cell results can be seen in the Table 1.

Table 1: Best cell IV results using two different front side metallization methods i.e. LCO+Plating and screen printing juxtaposed.

Emitter Type	Front Metal	η (%)	V_{oc} (mV)	J_{sc} (mA/cm²)	FF (%)
B3	LCO	22.2	680	40.2	81.3
B3	Screen Print	22.1	679	40.2	81.1
B2	LCO	22.2	675	40.0	82.0
B2	Screen Print	22.2	676	40.1	81.7

On an average, the Ni-Cu plating showed, for a screen printing optimized emitter (B2), a similar cell efficiency level compared to the screen printing reference group. The optimized processing sequence of LCO-FFO featured no laser-induced V_{oc} loss compared to the screen printing reference. Similar finger width and low contact resistances for both metallization technologies resulted in equal cell efficiencies for this emitter. The 150 Ω/sq. emitter of group B3 showed also similar V_{oc} level compared to screen printing. The plated cells, in some singular cases, show $0.1\%_{abs}$ efficiency gain in combination with B3 emitter profile in comparison to screen printed reference cells. Overall, no loss was seen in V_{oc} and an equal level of V_{oc}, Eta (η) and *FF* are achieved with laser and plating technology in comparison to screen printing.

4 CONCLUSIONS

We demonstrate the an efficiency advantage of $0{,}5\%_{abs}$ for laser ablated and Ni-Cu plated PERC solar cells caused by flipping the processing order from performing FFO before front side LCO to performing FFO after the front side LCO. The increased efficiency is due to higher V_{oc} and *pFF*. Therefore, we allocate the improvement in solar cells performance to recrystallization of laser damage after LCO and it warrants further deeper investigation into this phenomena.

5 ACKNOWLEDGEMENTS

This work has been performed under the aegis of project "Groschen" (FKZ: 0324012B), funded by German Federal Ministry for Economic Affairs and Energy.

The authors would also like to extend a word of thanks to HQC Cells GmbH for sharing their technology and precursors for testing at our facility and also for sharing the results.

6 REFERENCES

[1] M. Kamp, J. Bartsch, S. Nold, M. Retzlaff, M. Hörteis, and S. W. Glunz, "Economic evaluation of two-step metallization processes for silicon solar cells," *Energy Procedia*, vol. 8, pp. 558–564, 2011.

[2] A. ur Rehman and S. H. Lee, "Review of the potential of the Ni/Cu plating technique for crystalline silicon solar cells," *Materials (Basel).*, vol. 7, no. 2, pp. 1318–1341, 2014.

[3] S. Kluska *et al.*, "Electrical and Mechanical Properties of Plated Ni/Cu Contacts for Si Solar Cells," *Energy Procedia*, vol. 77, pp. 733–743, 2015.

[4] A. Büchler *et al.*, "Interface oxides in femtosecond laser structured plated Ni-Cu-Ag contacts for silicon solar cells," *Sol. Energy Mater. Sol. Cells*, vol. 166, no. March, pp. 197–203, 2017.

[5] M. Abbott, P. Cousins, F. Chen, and J. Cotter, "Laser-induced defects in crystalline silicon solar cells," *Conf. Rec. IEEE Photovolt. Spec. Conf.*, vol. 61, no. 0, pp. 1241–1244, 2005.

[6] G. Poulain *et al.*, "Characterization of laser-induced damage in silicon solar cells during selective ablation processes," *Mater. Sci. Eng. B Solid-State Mater. Adv. Technol.*, vol. 178, no. 9, pp. 682–685, 2013.

[7] C. Dang *et al.*, "Investigation of laser ablation induced defects in crystalline silicon solar cells," *Energy Procedia*, vol. 55, pp. 649–655, 2014.

[8] S. Steffens *et al.*, "Impact of dislocations and dangling bond defects on the electrical performance of crystalline silicon thin films," *Appl. Phys. Lett.*, vol. 105, no. 2, 2014.

[9] A. A. Brand, F. Meyer, J. F. Nekarda, and R. Preu, "Reduction of picosecond laser ablation threshold and damage via nanosecond pre-pulse for removal of dielectric layers on silicon solar cells," *Appl. Phys. A Mater. Sci. Process.*, vol. 117, no. 1, pp. 237–241, 2014.

[10] S. Rapp, G. Heinrich, M. Wollgarten, H. P. Huber, and M. Schmidt, "Physical mechanisms of SiNx layer structuring with ultrafast lasers by direct and confined laser ablation," *J. Appl. Phys.*, vol. 117, no. 10, pp. 1–9, 2015.

[11] P. Lorazo, L. J. Lewis, and M. Meunier, "Molecular-dynamics thermal annealing model of laser ablation of silicon," pp. 1–18, 2001.

[12] J. Koc, S.; Zavetova, M.; Zemek, "Physical Properties of Amorphous Si: The Role of Annealing," *Czechoslov. J. Phys.*, vol. 25, pp. 83–90, 1975.

[13] H. Bouridah, F. Mansour, R. Mahamdi, N. Bounar, and P. Temple-Boyer, "Effect of thermal annealing and nitrogen content on amorphous silicon thin-film crystallization," *Phys. Status Solidi Appl. Mater.*, vol. 204, no. 7, pp. 2347–2354, 2007.

[14] G. Marcins, J. Butikova, I. Tale, B. Polyakov, R. Kalendarjov, and A. Muhin, "Crystallization processes of amorphous Si by thermal annealing and pulsed laser processing," *IOP Conf. Ser. Mater. Sci. Eng.*, vol. 23, no. 1, 2011.

[15] S. Kluska et al. (2018) "Plated Fine Line Metallization for PERC Solar Cells". *35th EU-PVSEC*, to be published.